NANO LETTERS

Letter

pubs.acs.org/NanoLett

Surface Coating Constraint Induced Self-Discharging of Silicon Nanoparticles as Anodes for Lithium Ion Batteries

Langli Luo,[†] Peng Zhao,[‡] Hui Yang,[‡] Borui Liu,[§] Ji-Guang Zhang,[∥] Yi Cui,[⊥,#] Guihua Yu,[*,§] Sulin Zhang,[*,‡] and Chong-Min Wang[*,†]

[†]Environmental Molecular Sciences Laboratory, Pacific Northwest National Laboratory, 902 Battelle Boulevard, Richland, Washington 99352, United States

[‡]Engineering Science and Mechanics and Bioengineering, Pennsylvania State University, University Park, Pennsylvania 16801, United States

[§]Materials Science and Engineering Program and Department of Mechanical Engineering, The University of Texas at Austin, Austin, Texas 78712, United States

[∥]Energy and Environmental Directorate, Pacific Northwest National Laboratory, 902 Battelle Boulevard, Richland, Washington 99352, United States

[⊥]Department of Materials Science and Engineering, Stanford University, Stanford, California 94305, United States

[#]Stanford Institute for Materials and Energy Sciences, SLAC National Accelerator Laboratory, 2575 Sand Hill Road, Menlo Park, California 94025, United States

Supporting Information

ABSTRACT: One of the key challenges of Si-based anodes for lithium ion batteries is the large volume change upon lithiation and delithiation, which commonly leads to electrochemi-mechanical degradation and subsequent fast capacity fading. Recent studies have shown that applying nanometer-thick coating layers on Si nanoparticle (SiNPs) enhances cyclability and capacity retention. However, it is far from clear how the coating layer function from the point of view of both surface chemistry and electrochemi-mechanical effect. Herein, we use in situ transmission electron microscopy to investigate the lithiation/delithiation kinetics of SiNPs coated with a conductive polymer, polypyrrole (PPy). We discovered that this coating layer can lead to "self-delithiation" or "self-discharging" at different stages of lithiation. We rationalized that the self-discharging is driven by the internal compressive stress generated inside the lithiated SiNPs due to the constraint effect of the coating layer. We also noticed that the critical size of lithiation-induced fracture of SiNPs is increased from ~150 nm for bare SiNPs to ~380 nm for the PPy-coated SiNPs, showing a mechanically protective role of the coating layer. These observations demonstrate both beneficial and detrimental roles of the surface coatings, shedding light on rational design of surface coatings for silicon to retain high-power and high capacity as anode for lithium ion batteries.

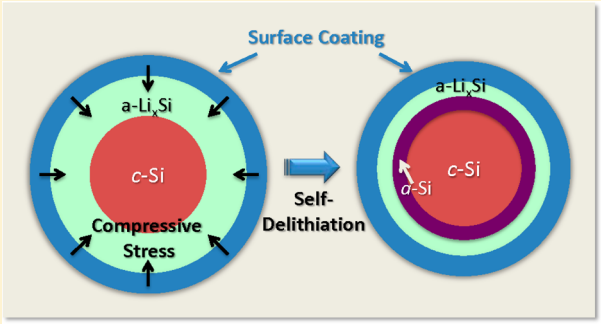

KEYWORDS: *Si anode, polymer coating, mechanical constraint, self-discharge*

Silicon is one of the most promising candidates for next-generation high-capacity anode for lithium ion batteries. However, the large volume change during charge/discharge cycles of Si anodes can cause disintegration of the active materials from other components, leading to direct system failure.[1] Since the revival of Si-based anodes, several strategies have been employed to design Si nanocomposites, including simple mixture,[2] surface coating,[3−5] 2D layer supporting,[6,7] porous,[8−11] core−shell,[12−14] and other 3D nanostructures,[10,15−22] which have successfully increased the cycle life of Si-based electrodes with improved capacity retention. Among these strategies, surface coatings have received much attention. The function of surface coating has been evaluated from distinctive aspects of both chemical and mechanical effect. Chemically, surface coatings have been perceived to act as protective layers that can mitigate unwanted continuous side reactions between Si and electrolytes during the charge and discharge cycles of the battery. Mechanically, surface coatings may provide confinements to ensure the integrity of Si electrodes and continuous electrical contact for enhanced electron and Li^+ conductivity, leading to improved cyclability, capacity retention, and high-power performance of Si based anodes.[23−28]

Received: August 1, 2015
Revised: September 17, 2015
Published: September 28, 2015

DOI: 10.1021/acs.nanolett.5b03047
Nano Lett. 2015, 15, 7016−7022

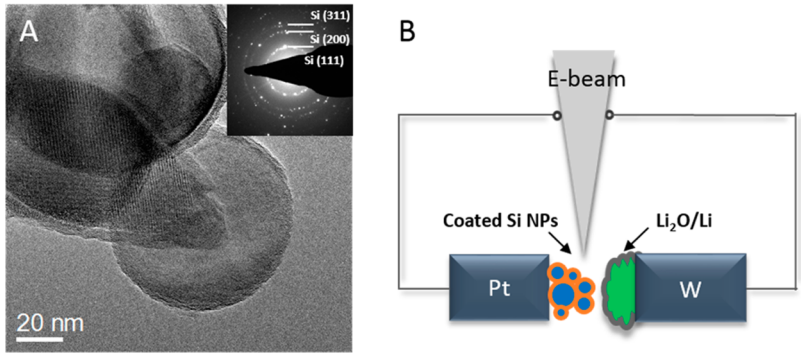

Figure 1. (A) Bright-field TEM images of a cluster of crystalline SiNPs coated with a layer of PPy. The inset is the SAED pattern of multiple crystalline SiNPs. (B) Schematic of a half-cell "nanobattery" in the TEM.

Despite large collections of research in surface-coated Si anodes focusing on materials processing and property characterization, fundamental understanding of how these surface coatings alter the lithiation/delithiation kinetics of Si nanostructures remains not fully understood. The in situ transmission electron microscopy (in situ TEM) techniques have enabled real-time imaging of dynamic compositional and microstructural evolutions during electrochemical reactions in electrodes,[29] providing insights into the lithiation/delithiation induced degradation mechanisms for a variety of anode materials including Si nanocomposites.[30−37] Herein, we report the role of surface coating, made of a conductive polymer, Polypyrrole (PPy), on the lithiation/delithiation kinetics of Si nanoparticles (SiNPs) via in situ TEM. We found that the constraint of the surface coating on the SiNPs can cause "self-delithiation" of the lithiated SiNPs, or "self-discharging" of the battery. We also noticed that the coated SiNPs with a size of ∼380 nm can survive the ultrafast lithiation without fracture, which is significantly larger than the observed critical diameter ∼150 nm of bare SiNPs.[38] These observations demonstrate both beneficial and detrimental effects of surface coatings on SiNPs in electrochemical reactions and provide insights on designing Si-based electrode system.

Figure 1A shows a high resolution TEM image of a cluster of *c*-SiNPs that were conformally coated with a layer of PPy of 5−10 nm in thickness, which differentiates them from the native oxide layer of SiNPs that usually has a thickness of typically ∼2 nm. The inset in Figure 1A shows the selected-area electron diffraction (SAED) pattern of several coated SiNPs, showing the typical *c*-Si ring pattern. As illustrated by the schematic in Figure 1B, these pristine PPy-coated SiNPs were suspended on the tip of a Pt rod and brought in contact with Li_2O covered Li metal on a W tip inside the TEM chamber. When applying a positive external voltage to the Li_2O/Li end, the Li ions are driven through Li_2O (working as a solid electrolyte) to alloy SiNPs, forming an amorphous Li_xSi phase. On the contrary, the Li ions can be extracted back to the Li_2O/Li end when applying a negative external voltage.

Figure 2 depicts the time-resolved bright-field TEM images captured from the Supporting Information video S1, showing the dynamic morphological changes of three PPy-SiNPs upon lithiation. Conductive polymer PPy with a thickness of ∼7 nm were conformably attached to the surface of SiNPs with a sharp interface (white dash line), as shown in Figure 2A. After 20 s of lithiation, two SiNPs started to expand and the newly formed *a*-Li_xSi phase was shown as bright contrast regions between PPy coatings and *c*-Si core in Figure 2B. The PPy coating expanded

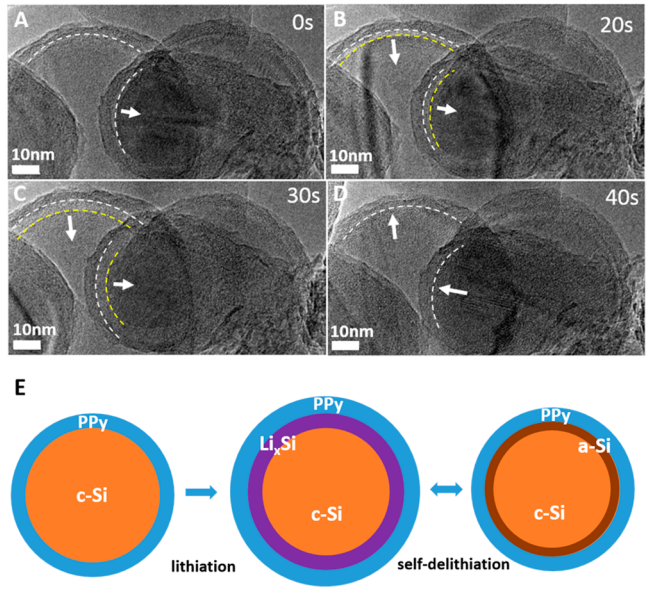

Figure 2. (A−D) Time-resolved TEM images depict the "fluctuation" of two SiNPs during lithiation process. White dash lines in Figure 4A,D indicate the interface between *c*-SiNP and PPy coating, and yellow dash lines in Figure 4B,C indicate the interface between *c*-Si core and *a*-Li_xSi shell. The white arrows show the moving directions of the interface. (E) Schematic of three stages during "fluctuation" lithiation of a coated SiNP.

along with SiNPs but remained adherent to the newly formed *a*-Li_xSi phase as the amorphous−crystalline interface (yellow dash line) propagated inward of the SiNPs. We noticed that following 30 s lithiation, the thickness of the *a*-Li_xSi layer increased to ∼7 nm (Figure 2C), the amorphous−crystalline interface stopped moving inward but surprisingly began to move backward, indicating a self-delithiation of the a-Li_xSi and this self-delithiation leads to the lithiated SiNPs to shrink to almost its original size with the *a*-Li_xSi phase diminished within 10 s. This "lithiation to self-delithiation" cycle, or "fluctuation lithiation/delithiation" repeated multiple times during the lithiation of this cluster of SiNPs, as illustrated in the schematic in Figure 2. The frequency of the fluctuation lithiation/delithiation varies from time to time, as shown in Supporting Information video S2, where fluctuation lithiation/delithiation occurred ten times during the course of the initial 40 s lithiation, and SiNPs "froze" in the next 40 s. This indicates that the fluctuation lithiation/delithiation was not caused by accidental oscillation of the applied external voltage for driving

DOI: 10.1021/acs.nanolett.5b03047
Nano Lett. 2015, 15, 7016−7022

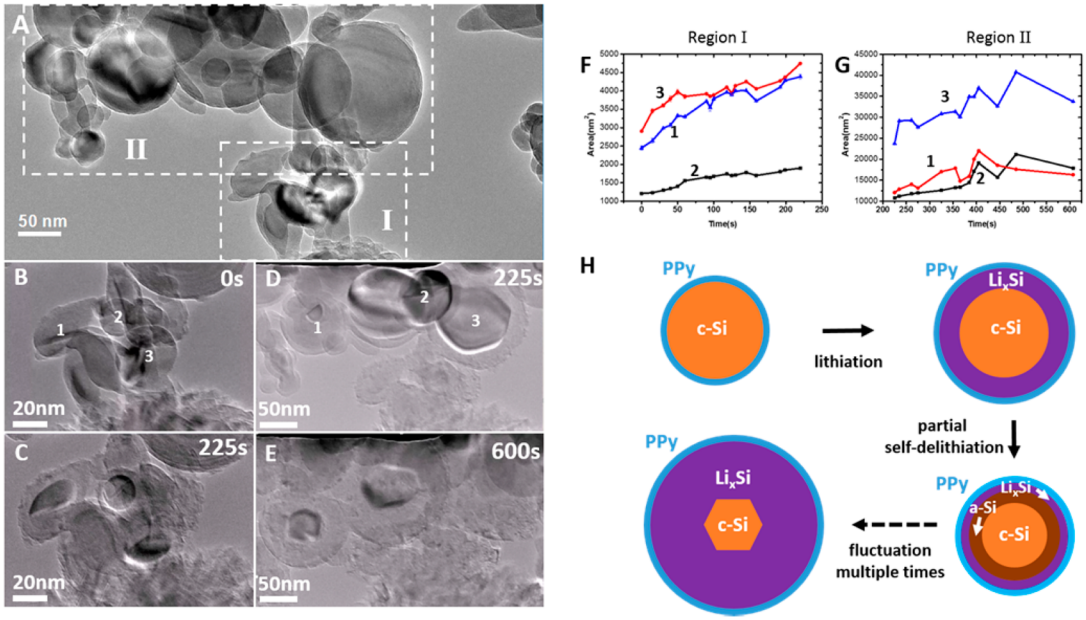

Figure 3. (A) Bright-field TEM image of pristine multiple PPy-coated SiNPs shows two regions of interest. (B,C) and (D,E) TEM images of PPy-coated SiNPs before and after lithiation for region I and II, respectively. (F,G) Projected area of SiNPs versus lithiation time for three SiNPs labeled as No. 1, 2, and 3 in region I and II are plotted to show the "fluctuation" lithiation process. (H) Schematic of the progressive "fluctuation" process.

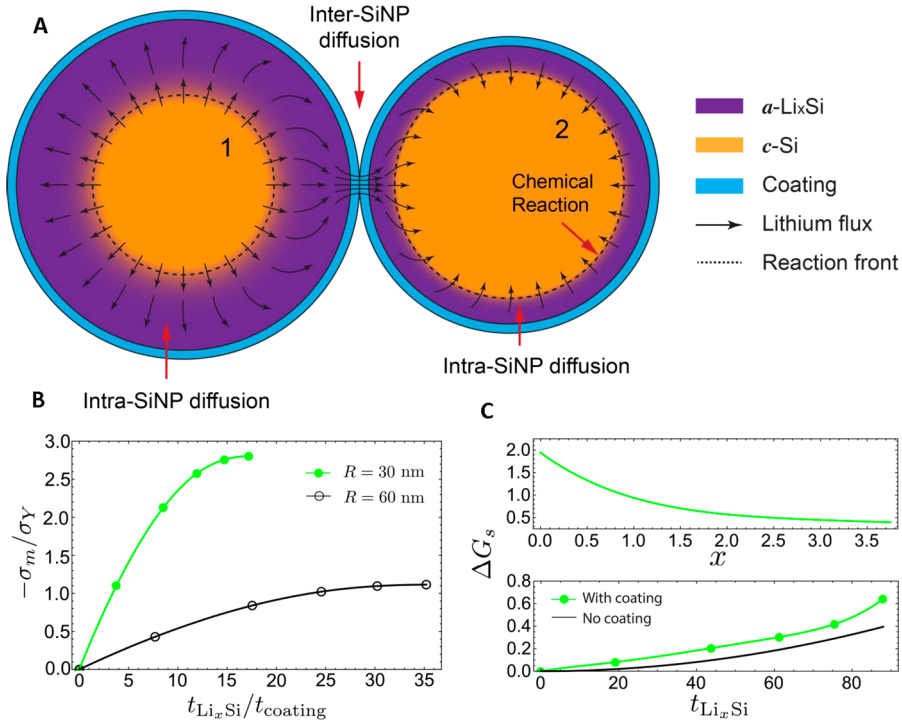

Figure 4. (A) Different stress states in the lithiated shells of neighboring SiNPs create a chemical potential gradient that drives inter-SiNP Li diffusion from 1 to 2. The outward Li diffusion from SiNP I dilutes Li concentration not only in the lithiated shell but also the reaction front, resulting a reduced driving force for chemical reaction that may lead to retroactive motion of the reaction front, that is, self-delithiation. At the same time, SiNP II is being lithiated. This process continues until the chemical potential of Li at the outer surfaces of the two neighboring SiNPs reaches a balance. (B) The mechanical confinement of surface coating generates large hydrostatic compressive stress at the outer surface of the lithiated SiNP (at the interface between the lithiated *a*-Li$_x$Si phase and the coating). The hydrostatic stress increases with lithiation depth. At the same lithiation depth, the smaller the SiNP, the higher the hydrostatic stress. In contrast, lithiation induces constant hydrostatic stress at the outer surface of uncoated SiNPs, regardless of the lithiation depth and SiNP size. (C) The free energy resisting chemical reaction, ΔG_S, increases with reduced lithium composition at the reaction front (top panel) and increased lithiation depth (bottom panel).

lithiation. Furthermore, this fluctuation lithiation/delithiation phenomenon is only present in the coated SiNPs, indicating the surface coating plays a critical role in the fluctuation, as described next. It should be noted that the PPy coating will be lithiated, which is accompanied by a volume increase. When the PPy is applied as a coating layer on Si nanoparticle, due to the

DOI: 10.1021/acs.nanolett.5b03047
Nano Lett. 2015, 15, 7016−7022

expansion of Si nanoparticle upon lithiation, the lithiated PPy layer is also stretched. Therefore, upon initial lithiation it seems that the PPy layer shows no significant change in thickness.

The above fluctuation lithiation/delithiation behavior on the three SiNPs cluster has also been noticed for clusters with a large number of SiNPs as illustrated in Figure 3. Because real electrodes constitute a large number of interconnected SiNPs, the electrochemical behavior of multiple SiNPs is more representative of the electrode. In Figure 3A, we focus on multiple SiNPs in two regions with small particle size (region I) and large one (region II). The lithiation processes of SiNPs in regions I and II are depicted in Supporting Information videos S3 and S4, respectively. As illustrated in the schematic of Figure 3H, lithiation proceeds when the lithiation front propagates toward the center of the SiNPs, but the lithiation depth fluctuates, rather than monotonically increases. The SiNPs was lithiated and followed by a slight self-delithiation of the lithiated phase, leading to the formation of an *a*-Si phase between the *c*-Si and *a*-Li_xSi phase. The slight self-delithiation is followed by the lithiation of the particles, indicating a progressive fluctuation lithiation/delithiation process for these two clusters of particles. The fluctuation lithiation/delithiation cycles repeated several times, leading to a much slower but progressive lithiation for the whole cluster of SiNPs. The initial and final lithiation profiles of the SiNPs in regions I and II are shown in Figure 3B,C and Figure 3D,E, respectively. The kinetics of this progressive fluctuant lithiation is indicated by the dynamic variation of the projected areas of the SiNPs in regions I and II (labeled as No. 1, 2, and 3), as plotted in Figure 3F,G. The fluctuation lithiation/delithiation cycles are shown clearly by several valleys on the curves. It is noted that the depth of these valleys is larger for large SiNPs (Figure 3G) than that for small SiNPs (Figure 3F). On the basis of electron beam blanking experiment, we confirm that the observed fluctuation lithiation/delithiation is not caused by electron beam effect.

The fluctuation lithiation/delithiation is originated from the constraint effect of the coating layer to the large volume expansion accompanying the lithiation of Si, as shown in Figure 4A. To elucidate the underlying mechanism, we begin with the stress-mediated driving forces for chemical reaction and Li diffusion in lithiation. Lithiation of Si is a process in series with chemical reaction at the reaction front, that is, amorphous–crystalline interface, and Li diffusion at the lithiated *a*-Li_xSi phase.[30,39,40] With externally applied voltage ϕ, the change in the Gibbs free energy ΔG_r serves as the driving force for the formation of $1/x$ units of Li_xSi in the chemical reaction at the reaction front[41]

$$\Delta G_r = \Delta G_r^0 - e\phi + \frac{1}{x}[\sigma_m^{Si}\Omega^{Si} - \sigma_m^{Li_xSi}\Omega^{Li_xSi}] \quad (1)$$

where ΔG_r^0 is the free energy change in the absence of mechanical stress and applied voltage, and ϕ is the voltage applied to the electrochemical cell. The free energy is related to the stress states of the phases across the reaction front, with σ_m^{Si} being the hydrostatic stress in the *c*-Si phase, and $\sigma_m^{Li_xSi}$ in the lithiated *a*-Li_xSi phase. Note that Ω^{Si} and Ω^{Li_xSi} are the corresponding unit volumes of the phases. The term $\Delta G_S \equiv 1/x[\sigma_m^{Si}\Omega^{Si} - \sigma_m^{Li_xSi}\Omega^{Li_xSi}]$ is the resistant force to the reaction, depending on both composition and stress state at the reaction front, as shown in Figure 4C. Typically, $\Delta G_S > 0$ in a compressed SiNP, which follows that compressive stress retards lithiation. In addition, ΔG_S is strongly dependent on the composition, x, or the local Li concentration $c = x/(1 + x)$. At a given stress state, ΔG_S increases when the Li concentration decreases. For a fairly low Li concentration behind the reaction front, ΔG_S may be sufficiently high to favor retroactive motion of the reaction front.

Li diffusion is driven by the gradient of chemical potential of Li. A general expression of the chemical potential of Li is

$$\mu = \mu_0 + kT \log\left[\frac{\gamma c}{(1 - c)}\right] - \Omega^{Li}\sigma_m^{Li_xSi} \quad (2)$$

where μ_0 is the reference chemical potential, Ω^{Li} is the partial volume of Li in the Li_xSi phase, kT is the thermal energy, and γ is the activity constant. From eq 2, one notes that Li diffusion can be driven by the Li concentration gradient or/and the stress gradient.[42−45] During lithiation, saturated Li at the surface of the SiNP diffuses inward to the reaction front, facilitating lithiation reaction. Meanwhile, the lithiation generated compressive stress in the *a*-Li_xSi phase slows down Li diffusion, which retards lithiation.[37,40,44−46]

The constraint of the coating causes buildup of compressive stress in the lithiated regions and at the reaction front as the SiNP swells, which modifies the driving force both for chemical reaction at the reaction front and the inter-SiNP diffusion, as shown in Figure 4B,C. Several possible reasons may lead to different levels of compressive stress buildup in neighboring SiNPs during lithiation, yielding different chemical potential of Li at the outer surface of the lithiated *a*-Li_xSi phase. First, the SiNPs may be unevenly lithiated, that is, lithiated by different depths, possibly due to the different local voltage applied to each individual SiNP. Second, SiNPs of different sizes may also build up different levels of compressive stress. When two such SiNPs with different stress states are brought into contact, inter-SiNP diffusion occurs, driven by the chemical potential gradient, even though their surfaces are equally supersaturated with Li, that is, with the same Li concentration at their surfaces. Without the loss of generality, we assume inter-SiNP diffusion occurs from SiNP I to SiNP II ($\Delta\mu = \mu_I - \mu_{II} > 0$). The inter-SiNP diffusion rapidly dilutes the Li concentration not only at the outer surface but also at the reaction front of SiNP I, leading to an increased ΔG_S. The free energy for chemical reaction may change its sign (from negative to positive), leading to the retroactive motion of the reaction front, that is, self-delithiation, in SiNP I, as schematically shown in Figure 4A. It is worth pointing out that self-delithiation does not occur in uncoated SiNPs. This is because the chemical potential gradient driving inter-SiNP diffusion vanishes between two lithiated uncoated SiNPs because the stress states at their lithiated outer surfaces are always the same ($\sigma_m = 2\sigma_Y/3$, where $\sigma_Y \sim 1.5$ GPa is the yielding stress.) regardless of the lithiation depth or their size.

Delithiation of SiNP I will lead to instantaneous lithiation of SiNP II. As this inter-SiNP diffusion continues, the compressive stress in SiNP I decreases, while that in SiNP II increases. Eventually the two SiNPs reach an isopotential, such that $\Delta\mu = 0$, and the inter-SiNP diffusion stops. The relatively low compressive stress is now insufficient to fully stall the lithiation of SiNP I. As a result, lithiation resumes and the reaction front moves forward in SiNP I. The lithiation-self-delithiation repeats when the above conditions are met at different stages of lithiation.

The constraint of the coating layer has also been found to have a strong effect on the behavior of the lithiated SiNPs after the removal of the external voltage. Essentially, the constraint of

DOI: 10.1021/acs.nanolett.5b03047
Nano Lett. 2015, 15, 7016−7022

the coating layer can lead to self-delithiation as illustrated in Figure 5. Figure 5A–C captured from Supporting Information

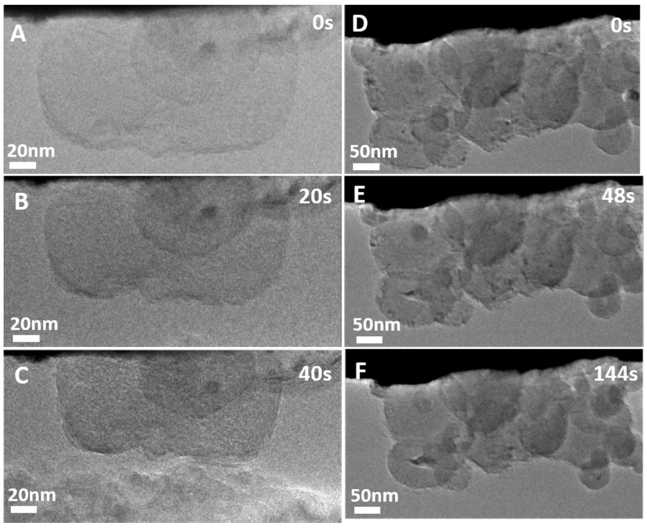

Figure 5. Time-resolved TEM images of "self-delithiation" process of a fully lithiated SiNP (A–C) and multiple SiNPs (D–F) after the removal of the external bias.

video S5 illustrates the "self-delithiation" process of single SiNP. Right after the second lithiation, the SiNP started to shrink in size. After 300 s, the lateral dimension of the SiNP decreased from 184 to 180 nm and the vertical size changed from 107 to 102 nm, corresponding to a volume change of ~8.77%, which accounts for 25% of its discharge capacity in the first cycle. Figure 5D–F captured from Supporting Information video S6 shows the "self-delithiation" of a cluster of SiNPs, leading to apparent size shrinkage within 144 s following the removal the applied voltage. The self-delithiation of both single SiNP and multiple SiNPs are due to stress-driven Li diffusion from the lithiated SiNPs, possibly to the counter electrode (Li metal) through the electrolyte. In stress-free conditions, the chemical potential of Li in Li metal is higher than in Li_xSi, which favors lithiation. However, with high-level compressive stress generated in the coated SiNPs the chemical potential of Li in the lithiated SiNPs may be well higher than that in Li metal, causing self-delithiation of the SiNPs. One of the interesting observations is that for some cases, as typically shown in the Supporting Informatino video S3 and video S4, the fluctuation lithiation/delithation appears to happen simultaneously for most of the particles within the cluster. Apparently, for the multiparticles system upon lithiation the relative motion of the particles within the cluster may lead to external driving voltage change or even interruption of lithium source, consequently leading to simultaneous fluctuation lithiation/delithiation of the particles in the cluster.

It has been reported that for uncoated SiNPs there exists a critical size of ~150 nm beyond which the surface fracture would occur due to the large hoop tension generated at the outer surface of the lithiated SiNPs.[38] The constraint of the coating layer will act mechanically to decrease the tensile stress of the particle, therefore suppressing the pulverization of the SiNPs. Figure 6A–C shows the lithiation process of a large (~380 nm in diameter) PPy-coated SiNP. After 185 s of lithiation, the measured sizes increased from 386 to 565 nm laterally, and 392 to 432 nm vertically, corresponding to a total

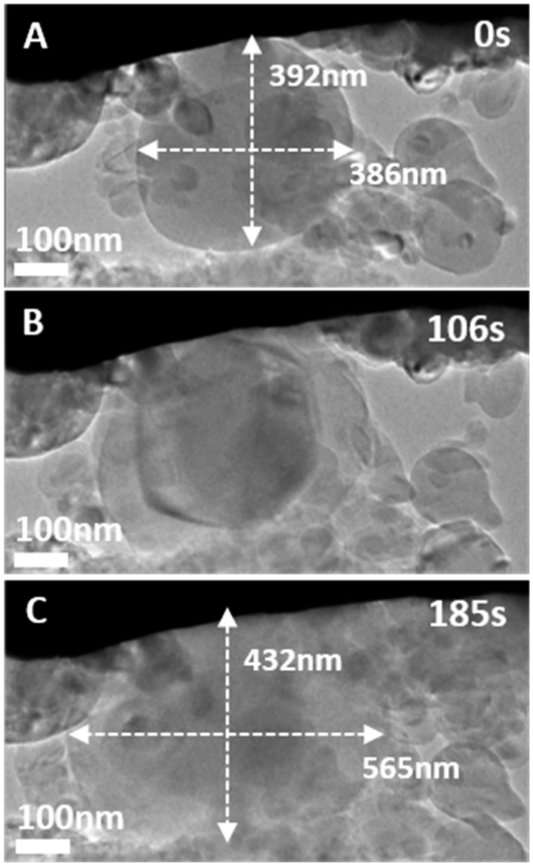

Figure 6. Time-resolved bright-field TEM images depict the lithiation process of a large (~380 nm in diameter) *c*-SiNP, showing that the SiNP undergoes a total volume expansion of 265% without fracture.

volume expansion of ~265%. As shown in Figure 6B, instead of generating hoop tension at the outer surface as seen in uncoated SiNPs, compressive stress is generated, which suppresses surface cracking. From the compressive stress state of the coated SiNPs, one reveals that fracture of the SiNP may only occur after the breakage of the surface coating.

In a more general term, it is beneficial to discuss the surface coating effect on the lithiation of crystalline Si in terms of the characteristics of the coating layer. Surface coatings are expected to function in multiple roles: First, they act as a protective layer that can mitigate the unwanted and continuous side reactions between Si and electrolytes. Second, a conductive coating layer can ensure good electronic and/or ionic contact during cycling. Third, the coating layer acts as a mechanical confinement that buffers the volume change of the anode during cycling.[33] Fourth, the constraint of the coating layer generates compressive stress, retarding lithiation or even causes self-discharging, as observed in this work. As seen from Figure 7, we can categorize four possible surface coatings on SiNPs to illustrate the guidelines for designing an effective surface coating. Column A shows a very hard or thick coating, which dramatically impedes the lithiation process or even causes lithiation stalling. Column B represents the coating layer that is brittle in nature, which fragments during the first lithiation and loses its function in the subsequent cycles of the battery. These two types of coatings are unwanted in the surface modification of SiNPs. Column C illustrates the case of a coating layer of a strong resilience, which will lead to a strong residual stress and can cause self-delithiation of Si, as reported in this paper.

DOI: 10.1021/acs.nanolett.5b03047
Nano Lett. 2015, 15, 7016–7022

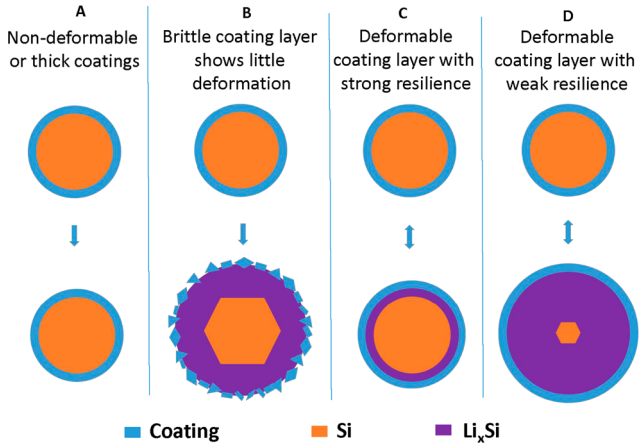

Figure 7. Schematic drawings to illustrate the effect of surface coatings on lithiation behavior. (A) Extremely hard or thick coatings lead to no lithiation. (B) Brittle coating leads to break of the surface coating during the lithiation. (C) Deformable coating with strong resilience that will lead to alternation of lithiation kinetics. (D) Deformable coating with weak resilience that will have weak retardation to lithiation.

However, by tuning the mechanical and chemical properties, a more effective coating can be developed, which retains the above-mentioned beneficial functions but suppresses the adverse effects, as illustrated in column D. It should be pointed out that what we have discussed in Figure 7 regarding the coating layer effect is only evaluated from the point of view of electrochemi-mechanical effect upon lithiation. The coating layer illustrated in D appears to be ideal in terms of electrochemi-mechanical effect, and the coupling of surface chemical effect will complicate the selection of coating layer.

CONCLUSIONS

The effect of surface coating on SiNPs on battery performance can be evaluated from the point of view of both electrochemical and mechanical effects. In this work, we investigated the lithiation kinetics and lithiation induced chemo-mechanical fracture of PPy-coated *c*-SiNPs. Our in situ TEM studies along with chemo-mechanical analyses reveal that the surface coating functions in both beneficial and detrimental roles for SiNPs as anodes. Owing to the constraint effect of the coating layer, large compressive stress may be generated both at the reaction front and in the lithiated shell, which not only retards lithiation, but also causes fluctuant lithiation/delithiation, leading to self-discharge of the battery. On the other hand, the coating layer acts as a mechanical confinement that buffers the volume change of the anode during cycling, rendering the SiNP electrochemi-mechanically more durable. Our findings suggest the significance of the coupled electrochemi-mechanical effects of surface coatings in the design of high-performance Si-based anodes for lithium ion batteries.

ASSOCIATED CONTENT

Supporting Information

The Supporting Information is available free of charge on the ACS Publications website at DOI: 10.1021/acs.nanolett.5b03047.

Description of the material. (PDF)

"Fluctuation" lithiation of PPy-coated SiNPs under bias of −3 V. The frame speed is 4× times of the real time. (AVI)

"Fluctuation" lithiation of PPy-coated SiNPs under bias of −3 V presents variable fluctuation frequency. The frame speed is 4× times of the real time. (AVI)

"Progressive Fluctuation" lithiation of a cluster PPy-coated SiNPs (Zone I) under bias of −3 V. The frame speed is 8× times of the real time. (AVI)

"Progressive Fluctuation" lithiation of a cluster PPy-coated SiNPs (Zone II) under bias of −3 V. The frame speed is 16× times of the real time. (AVI)

Self-delithiation process of a single PPy-coated SiNP without bias. The frame speed is 4× times of the real time. (AVI)

Self-delithiation process of multiple PPy-coated SiNPs without bias. The frame speed is 4× times of the real time. (AVI)

AUTHOR INFORMATION

Corresponding Authors

*E-mail: ghyu@austin.utexas.edu.
*E-mail: suz10@psu.edu.
*E-mail: Chongmin.Wang@pnnl.gov.

Author Contributions

L.L and P.Z. contributed equally to this paper.

Notes

The authors declare no competing financial interest.

ACKNOWLEDGMENTS

This work at PNNL and Stanford is supported by the Assistant Secretary for Energy Efficiency and Renewable Energy, Office of Vehicle Technologies of the U.S. Department of Energy under Contract No. DE-AC02-05CH11231, Subcontract No. 18769 and DE-AC-36-08GO28308 under the Advanced Batteries Materials Research (BMR). The in situ microscopic study described in this paper is supported by the Laboratory Directed Research and Development Program as part of the Chemical Imaging Initiative at Pacific Northwest National Laboratory (PNNL). The work was conducted in the William R. Wiley Environmental Molecular Sciences Laboratory (EMSL), a national scientific user facility sponsored by DOE's Office of Biological and Environmental Research and located at PNNL. PNNL is operated by Battelle for the DOE under Contract DE-AC05-76RLO1830. H.Y. and S.L.Z acknowledge the support by the NSF-CMMI (Grant 0900692). G.Y. acknowledges the financial support from National Science Foundation (CMMI-1537894) and 3M Nontenured Faculty Award.

REFERENCES

(1) Besenhard, J. O.; Yang, J.; Winter, M. *J. Power Sources* **1997**, *68* (1), 87−90.
(2) Li, H.; Huang, X.; Chen, L.; Wu, Z.; Liang, Y. *Electrochem. Solid-State Lett.* **1999**, *2* (11), 547−549.
(3) Yoshio, M.; Wang, H.; Fukuda, K.; Umeno, T.; Dimov, N.; Ogumi, Z. *J. Electrochem. Soc.* **2002**, *149* (12), A1598−A1603.
(4) Dimov, N.; Kugino, S.; Yoshio, M. *Electrochim. Acta* **2003**, *48* (11), 1579−1587.
(5) Hu, Y. S. *Angew. Chem., Int. Ed.* **2008**, *47*, 1645−1649.
(6) Lee, J. K.; Smith, K. B.; Hayner, C. M.; Kung, H. H. *Chem. Commun.* **2010**, *46* (12), 2025−2027.

DOI: 10.1021/acs.nanolett.5b03047
Nano Lett. 2015, 15, 7016−7022

(7) Evanoff, K.; Magasinski, A.; Yang, J. B.; Yushin, G. *Adv. Energy Mater.* **2011**, *1*, 495−498.
(8) Kim, H. J.; Han, B. H.; Choo, J. B.; Cho, J. *Angew. Chem., Int. Ed.* **2008**, *47*, 10151−10154.
(9) Ge, M. Y.; Rong, J. P.; Fang, X.; Zhou, C. W. *Nano Lett.* **2012**, *12*, 2318−2323.
(10) Gowda, S. R. *Nano Lett.* **2012**, *12*, 6060−6065.
(11) Jia, H.; Gao, P.; Yang, J.; Wang, J.; Nuli, Y.; Yang, Z. *Adv. Energy Mater.* **2011**, *1* (6), 1036−1039.
(12) Hwang, T. H.; Lee, Y. M.; Kong, B. S.; Seo, J. S.; Choi, J. W. *Nano Lett.* **2012**, *12*, 802−807.
(13) Jeong, G.; Kim, J.-G.; Park, M.-S.; Seo, M.; Hwang, S. M.; Kim, Y.-U.; Kim, Y.-J.; Kim, J. H.; Dou, S. X. *ACS Nano* **2014**, *8* (3), 2977−2985.
(14) Li, X.; Meduri, P.; Chen, X.; Qi, W.; Engelhard, M. H.; Xu, W.; Ding, F.; Xiao, J.; Wang, W.; Wang, C.; Zhang, J.-G.; Liu, J. *J. Mater. Chem.* **2012**, *22* (22), 11014−11017.
(15) Yao, Y.; McDowell, M. T.; Ryu, I.; Wu, H.; Liu, N.; Hu, L.; Nix, W. D.; Cui, Y. *Nano Lett.* **2011**, *11* (7), 2949−2954.
(16) Luo, J.; Zhao, X.; Wu, J.; Jang, H. D.; Kung, H. H.; Huang, J. *J. Phys. Chem. Lett.* **2012**, *3* (13), 1824−1829.
(17) Zhang, H. G.; Braun, P. V. *Nano Lett.* **2012**, *12*, 2778−2783.
(18) Chang, J.; Huang, X.; Zhou, G.; Cui, S.; Hallac, P. B.; Jiang, J.; Hurley, P. T.; Chen, J. *Adv. Mater.* **2014**, *26* (5), 758−764.
(19) Chen, X.; Li, X.; Ding, F.; Xu, W.; Xiao, J.; Cao, Y.; Meduri, P.; Liu, J.; Graff, G. L.; Zhang, J.-G. *Nano Lett.* **2012**, *12* (8), 4124−4130.
(20) Liu, N.; Lu, Z.; Zhao, J.; McDowell, M. T.; Lee, H.-W.; Zhao, W.; Cui, Y. *Nat. Nanotechnol.* **2014**, *9* (3), 187−192.
(21) Hu, L.; Liu, N.; Eskilsson, M.; Zheng, G.; McDonough, J.; Wågberg, L.; Cui, Y. *Nano Energy* **2013**, *2* (1), 138−145.
(22) Hassan, F. M.; Chabot, V.; Elsayed, A. R.; Xiao, X.; Chen, Z. *Nano Lett.* **2014**, *14* (1), 277−283.
(23) Yen, Y.-C.; Chao, S.-C.; Wu, H.-C.; Wu, N.-L. *J. Electrochem. Soc.* **2009**, *156* (2), A95−A102.
(24) Magasinski, A.; Zdyrko, B.; Kovalenko, I.; Hertzberg, B.; Burtovyy, R.; Huebner, C. F.; Fuller, T. F.; Luzinov, I.; Yushin, G. *ACS Appl. Mater. Interfaces* **2010**, *2* (11), 3004−3010.
(25) Nguyen, H. T.; Zamfir, M. R.; Duong, L. D.; Lee, Y. H.; Bondavalli, P.; Pribat, D. *J. Mater. Chem.* **2012**, *22* (47), 24618−24626.
(26) Wu, H.; Yu, G.; Pan, L.; Liu, N.; McDowell, M. T.; Bao, Z.; Cui, Y. *Nat. Commun.* **2013**, *4*, 1943.
(27) Liu, B.; Soares, P.; Checkles, C.; Zhao, Y.; Yu, G. H. *Nano Lett.* **2013**, *13*, 3414−3419.
(28) Zhao, Y.; Liu, B. R.; Pan, L. J.; Yu, G. H. *Energy Environ. Sci.* **2013**, *6*, 2856−2870.
(29) Huang, J. Y.; Zhong, L.; Wang, C. M.; Sullivan, J. P.; Xu, W.; Zhang, L. Q.; Mao, S. X.; Hudak, N. S.; Liu, X. H.; Subramanian, A.; Fan, H.; Qi, L.; Kushima, A.; Li, J. *Science* **2010**, *330* (6010), 1515−1520.
(30) Liu, X. H.; Wang, J. W.; Huang, S.; Fan, F.; Huang, X.; Liu, Y.; Krylyuk, S.; Yoo, J.; Dayeh, S. A.; Davydov, A. V.; Mao, S. X.; Picraux, S. T.; Zhang, S.; Li, J.; Zhu, T.; Huang, J. Y. *Nat. Nanotechnol.* **2012**, *7* (11), 749−756.
(31) McDowell, M. T.; Lee, S. W.; Nix, W. D.; Cui, Y. *Adv. Mater.* **2013**, *25* (36), 4966−4985.
(32) He, Y.; Piper, D. M.; Gu, M.; Travis, J. J.; George, S. M.; Lee, S.-H.; Genc, A.; Pullan, L.; Liu, J.; Mao, S. X.; Zhang, J.-G.; Ban, C.; Wang, C. *ACS Nano* **2014**, *8*, 11816.
(33) Luo, L.; Yang, H.; Yan, P.; Travis, J. J.; Lee, Y.; Liu, N.; Molina Piper, D.; Lee, S.-H.; Zhao, P.; George, S. M.; Zhang, J.-G.; Cui, Y.; Zhang, S.; Ban, C.; Wang, C.-M. *ACS Nano* **2015**, *9*, 5559.
(34) Ghassemi, H.; Au, M.; Chen, N.; Heiden, P. A.; Yassar, R. S. *ACS Nano* **2011**, *5* (10), 7805−7811.
(35) Bogart, T. D.; Lu, X.; Gu, M.; Wang, C.; Korgel, B. A. *RSC Adv.* **2014**, *4* (79), 42022−42028.
(36) McDowell, M. T.; Ryu, I.; Lee, S. W.; Wang, C.; Nix, W. D.; Cui, Y. *Adv. Mater.* **2012**, *24* (45), 6034−6041.
(37) Liu, X. H.; Fan, F.; Yang, H.; Zhang, S.; Huang, J. Y.; Zhu, T. *ACS Nano* **2012**, *7* (2), 1495−1503.
(38) Liu, X. H.; Zhong, L.; Huang, S.; Mao, S. X.; Zhu, T.; Huang, J. Y. *ACS Nano* **2012**, *6* (2), 1522−1531.
(39) Yang, H.; Huang, S.; Huang, X.; Fan, F.; Liang, W.; Liu, X. H.; Chen, L.-Q.; Huang, J. Y.; Li, J.; Zhu, T.; Zhang, S. *Nano Lett.* **2012**, *12* (4), 1953−1958.
(40) Yang, H.; Fan, F.; Liang, W.; Guo, X.; Zhu, T.; Zhang, S. *J. Mech. Phys. Solids* **2014**, *70*, 349−361.
(41) Zhao, K.; Pharr, M.; Wan, Q.; Wang, W. L.; Kaxiras, E.; Vlassak, J. J.; Suo, Z. *J. Electrochem. Soc.* **2012**, *159* (3), A238−A243.
(42) Grantab, R.; Shenoy, V. B. *J. Electrochem. Soc.* **2012**, *159* (5), A584−A591.
(43) Yang, H.; Huang, X.; Liang, W.; van Duin, A. C. T.; Raju, M.; Zhang, S. *Chem. Phys. Lett.* **2013**, *563*, 58−62.
(44) Gu, M.; Yang, H.; Perea, D. E.; Zhang, J.-G.; Zhang, S.; Wang, C.-M. *Nano Lett.* **2014**, *14* (8), 4622−4627.
(45) Yang, H.; Liang, W.; Guo, X.; Wang, C.-M.; Zhang, S. *Extreme Mech. Lett.* **2015**, *2*, 1−6.
(46) Liang, W.; Yang, H.; Fan, F.; Liu, Y.; Liu, X. H.; Huang, J. Y.; Zhu, T.; Zhang, S. *ACS Nano* **2013**, *7* (4), 3427−3433.

DOI: 10.1021/acs.nanolett.5b03047
Nano Lett. 2015, 15, 7016−7022